

Column Water Vapor from Diffuse Irradiance

*P. W. Kiedron, J. L. Berndt, L. C. Harrison, J. J. Michalsky, and Q.-L. Min
Atmospheric Sciences Research Center
State University of New York
Albany, New York*

Abstract

A possibility of measuring water vapor column from diffuse irradiance, and thus the extension of optical retrievals to cloudy days, was investigated. The data from the Rotating Shadowband Spectroradiometer (RSS) during its winter deployment at the North Slope of Alaska (NSA) site is used. The initial analysis covers 20 days in March 1999 that include clear, partly cloudy, and overcast days. During these days, water vapor column according to the NSA site's Microwave Radiometer (MWR) varied between 1 and 5 mm. The diffuse irradiances in the 820 and 940-nm water vapor absorption bands are compared with water vapor column obtained from the MWR. While these irradiances do not correlate well with the water vapor column, we found that by using the diffuse transmittance in the 760-nm oxygen absorption band to obtain an effective air mass, we could derive a method that greatly increases the correlation. The end result is a correlation of 0.97 and 0.95 between MWR and diffuse RSS retrievals using 820 and 940-nm transmittances, respectively. This encouraging result is based on empirical data analysis only. It implies that the diffuse irradiance may contain sufficient information to retrieve water vapor column. However, we must analyze broader data sets to ensure that the resulting high correlation in these data is not predicated on the limited climatological conditions experienced in March 1999 at the NSA site.

Introduction

The Intensive Operational Period (IOP) was conducted during the late winter/early spring of 1999 at the NSA Atmospheric Radiation Measurement (ARM) Program site near Barrow, Alaska, to compare various techniques to retrieve water vapor column in dry conditions. The RSS, deployed by the Atmospheric Sciences Research Center, was the only sun photometer taking part in this experiment. In addition to the 23.8 GHz-MWR, National Oceanic and Atmospheric Administration (NOAA) Environmental Technology Laboratory and National Aeronautics and Space Administration (NASA) Goddard Space Flight Center deployed two radiometers covering the 183-GHz band. The results of retrievals with MWRs can be found in Racette et al. (2000) and Westwater et al. (2000). The comparison between the optical and microwave methods was limited to 11 days of clear and semi-clear weather when solar direct beam measurements and retrievals could be performed. Figure 1, reproduced from Kiedron et al. (in print), shows a good agreement between optical and microwave measurements.

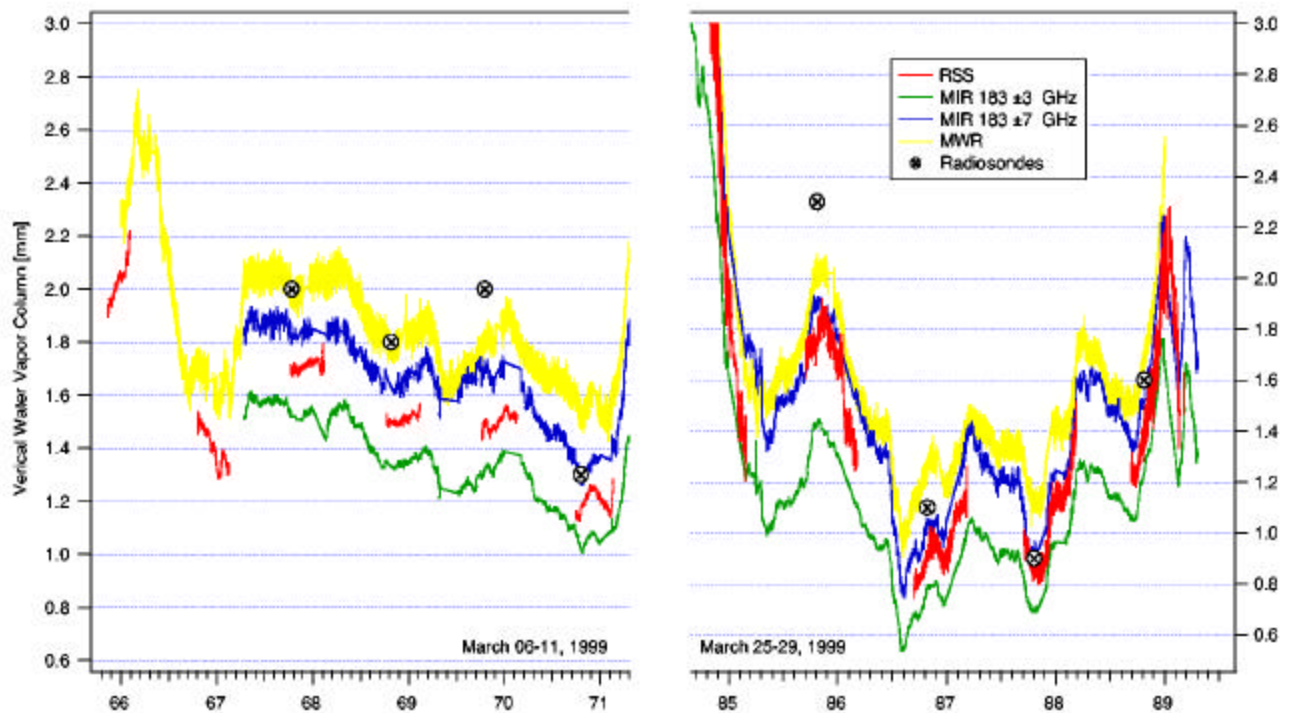


Figure 1. Comparison of water vapor retrievals with microwave radiometers and with direct beam RSS data on clear and semi-clear days.

The RSS provides continuous direct irradiance spectra over 512 pixels covering the wavelengths 350 - 1080 nm (see Harrison et al. 1999). This allows us to derive better estimates of transmittance at water absorption bands than with the filter spectroradiometers. A baseline is defined by the irradiance at neighboring wavelengths. Then a good estimate of irradiance at the absorption band, as if there were no water, is calculated. After the baseline is removed from the irradiance, the transmittance at the water absorption band is greatly desensitized to aerosols and radiometric calibration uncertainties. This method allows one to retrieve water vapor column even when the sun is partially obscured, or in the presence of fog, when only a fraction of direct beam can reach the instrument. But beyond some degree of direct beam extinction, the low signal-to-noise ratio makes retrievals impossible.

In addition to the direct horizontal irradiance, the RSS also measures the diffuse irradiance. The latter is provided even during overcast conditions or for very large solar zenith angles and has relatively high signal-to-noise ratio. In this paper, we explore the possibility of using the diffuse irradiance to retrieve the water vapor column.

Methodology

We try to find a function of diffuse irradiance that predicts the water vapor column retrieved by the MWR. More precisely, we concentrate on only two spectral elements of the diffuse irradiance: one at the water absorption band near 940 nm or 820 nm and the second at the oxygen absorption band near 760 nm. Mathematically speaking, we try to show that two spectral elements from diffuse irradiance

produce a result that correlates with water vapor column from the MWR measurement. In other words, we create an estimator F of water vapor column w :

$$w = F(I_{\text{dif}}(\lambda), I_{\text{dif}}(760), \bar{x}) \quad (1)$$

where $\lambda = 940 \text{ nm}$ or $\lambda = 820\text{-nm}$ and \bar{x} is the vector of parameters that are derived through the process that minimizes residuals $r = w - w_{\text{MWR}}$.

To eliminate sensitivity to aerosols and radiometric calibration errors, transmittances, instead of irradiances, at water and oxygen absorption bands are used. The irradiance is divided by the extraterrestrial and the baseline is removed. In Figure 2 we show diffuse irradiance divided by the extraterrestrial irradiance. The anchor points for each band's baseline are indicated. The value of the baseline at absorption wavelength λ is interpolated using values at anchor points λ_1 and λ_2 with the formula

$$B(\lambda) = I_{\text{dif}}(\lambda_1) \left(\frac{I_{\text{dif}}(\lambda_2)}{I_{\text{dif}}(\lambda_1)} \right)^{\frac{\lambda - \lambda_1}{\lambda_2 - \lambda_1}} \quad (2)$$

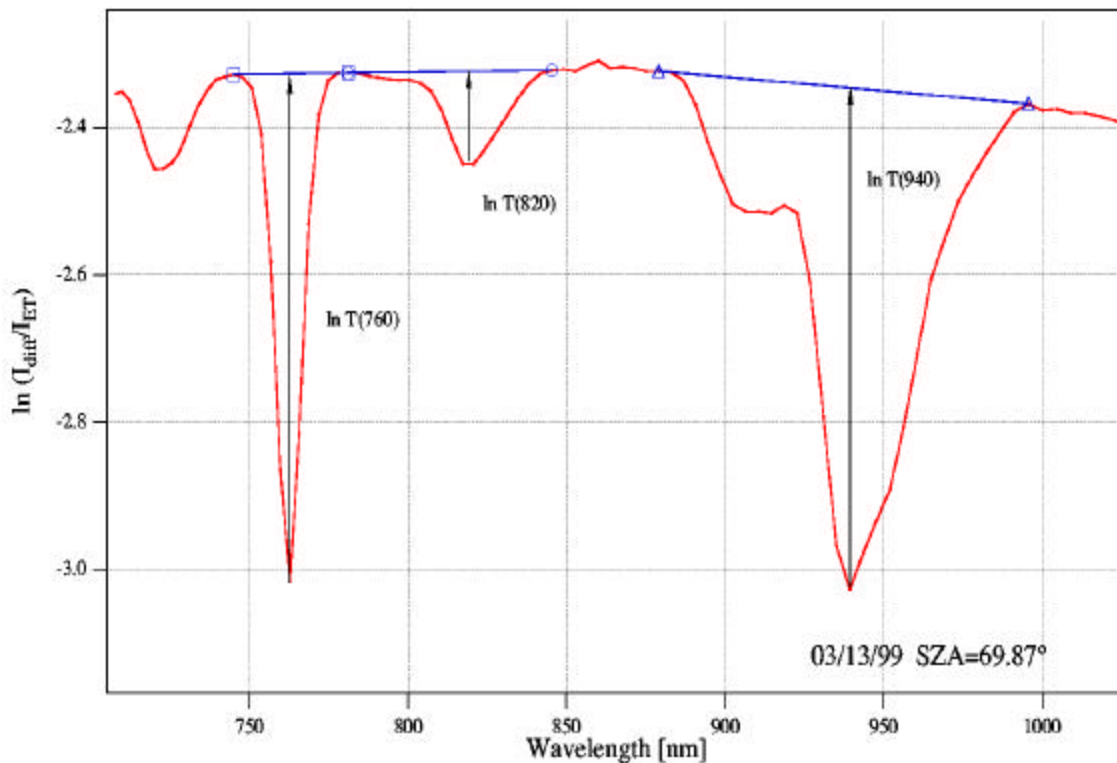


Figure 2. Example of diffuse irradiance. The anchor points used to define baselines for each absorption band are marked.

Then the transmittance at absorption wavelength is given by

$$T_{\text{dif}}(\lambda) = I_{\text{dif}}(\lambda) / B(\lambda) \quad (3)$$

The inclusion of irradiance at the oxygen absorption band has the following rationale. The oxygen profile and its total column are invariant. Thus, the absorption at oxygen band is dependent on geometry only and independent of variable atmospheric constituents and parameters. By incorporating the diffuse irradiance at 760 nm we hope to compensate for the effects of varying pathlength with different atmospheric conditions as well as with the varying sun position. For the same reason, high-resolution measurements at 760-nm band have been used and proposed to estimate the optical photon pathlength (Veitel et al. 1998; Pfeilsticker et al. 1998; Min and Harrison 1999). The estimator F will have no explicit dependence on time or on the solar zenith angle.

For the solar direct beam, the air mass is related to the transmittance at 760 nm through a curve of growth:

$$m = g(T_{\text{dir}}(760)) \quad (4)$$

Once the function $g()$ is established, we define the effective diffuse air mass as

$$m^* = g(T_{\text{dir}}(760)) \quad (5)$$

Next, we try to find the functional relationship between the diffuse transmittance and the product of the water vapor column and the effective diffuse air mass

$$w_{\text{MWR}} \cdot m^* = h(T_{\text{dif}}(\lambda)) \quad (6)$$

where $\lambda = 820$ nm or $\lambda = 940$ nm. The function $h()$ is found in the least square sense by minimizing the root mean square (rms) difference between the two sides of Eq. (6). The $h()$ can be looked at as a curve of growth relating equivalent diffuse water column $w_{\text{MWR}}m^*$ to diffuse transmittance. For this reason, we try to fit a function that can have a physical interpretation as a curve of growth.

Finally, from Eqs. (5) and (6) one can define the estimator of water vapor column as follows:

$$w = \frac{h(T_{\text{dif}}(\lambda))}{g(T_{\text{dif}}(940))} \quad (7)$$

The quality of the estimator (7) is measured with the correlation coefficient and the rms error between w and w_{MWR} .

Curve of Growth Model

We used Moskalkenko's (1969) model of the curve of growth for both functions $g()$ and $h()$; however, we must emphasize that the selection of the model function is not essential to our task. In fact, to establish correlation between diffuse transmittance and water vapor column, functions $g()$ and $h()$ were originally expressed with polynomials. Now, by using a curve of growth with parameters that may have a physical interpretation, we hope to facilitate tying our results with future model calculations.

Moskalkenko's model relates transmittance to the air mass $x = m$ or $x = w_{MWR}m^*$ as follows:

$$\ln T = -k \cdot x^{f(x)} \quad (8)$$

where $f(x)$ varies between 1 and 1/2. We chose $f(x)$ in the following form

$$f(x) = 1 - a \frac{x}{x + b} \quad (9)$$

with two positive parameters a and b . Always $f(0) = 1$ and $f(\bullet) = 1 - a$. However, we did not limit a to assure the physical condition $f(\bullet) > 0.5$. To obtain values of $x = g(T)$ or $x = h(T)$, Eq. (8) was solved numerically with respect to x .

Results

The 20-day data set totals over 12,000 diffuse and direct irradiance spectra. Among the data six days were clear. We added data from two clear days in April to generate the curve of growth $g()$ from the direct transmittance at 760 nm. In Figure 3 the air mass according to Kasten (1965) is plotted against the logarithm of transmittance. The residuals show several systematic tendencies of which one remains unexplained. We do not know why data from four days cluster above the best-fit curve and from the remaining four days below the curve. The sudden step change in residuals for low air masses is due to non-linearity in the RSS's NMOS array after exposure changes. The increase of residuals for large air masses is due to the lower signal-to-noise ratio for large solar zenith angles. The morning and afternoon branches for each day coincide, implying that RSS's time keeping is accurate. In summary, the residuals are still within ± 2 percent for small and medium air masses and ± 4 percent for large air masses. The curves of growth $h()$ for diffuse transmittances at 820 nm and 940 nm are derived in Figure 4. It is evident that the outliers are not random. This suggests a need for an additional parameterization. Nevertheless, for each data point, we calculate two estimates of water vapor column with Eq. (7). The results are presented in two correlation plots in Figure 5 and in Figure 6 as a function time.

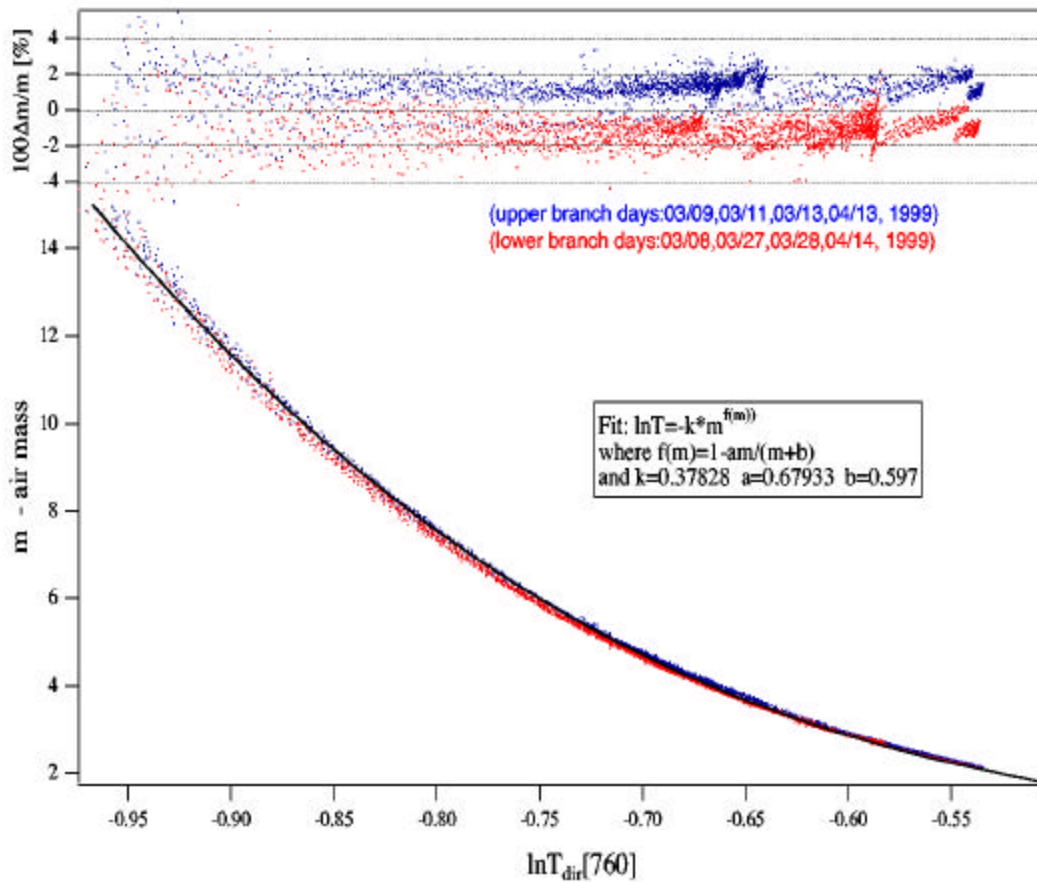


Figure 3. Empirical derivation of curve of growth at 760 nm.

Discussion

The correlation of 0.97 and 0.95 between MWR and diffuse RSS retrievals using 820-nm and 940-nm transmittances, respectively, can be considered very high. We speculate that the retrievals with 820 nm are slightly better because of the fact that the 820-nm photons travel a more similar path to the 760-nm photons than the 940-nm photons.

The retrieval errors have a random component with zero mean and a systematic component:

$$\bullet W = \bullet W_{RND} + \bullet W_{SYST} \quad (10)$$

The random error is particularly large on clear days $jd = 77, 78, 87,$ and 88 (see Figure 6). This is because the shadowbanding cycle of RSS is performed with one fixed exposure that is determined at the beginning of the cycle by the signal of unblocked measurement that must be kept below the detector saturation point. In consequence, the blocked signal that determines the diffuse irradiance is measured at too low an exposure during clear-sky days. This error can be reduced by averaging data points or by implementing a change in RSS firmware to perform the blocked measurement at maximal exposure.

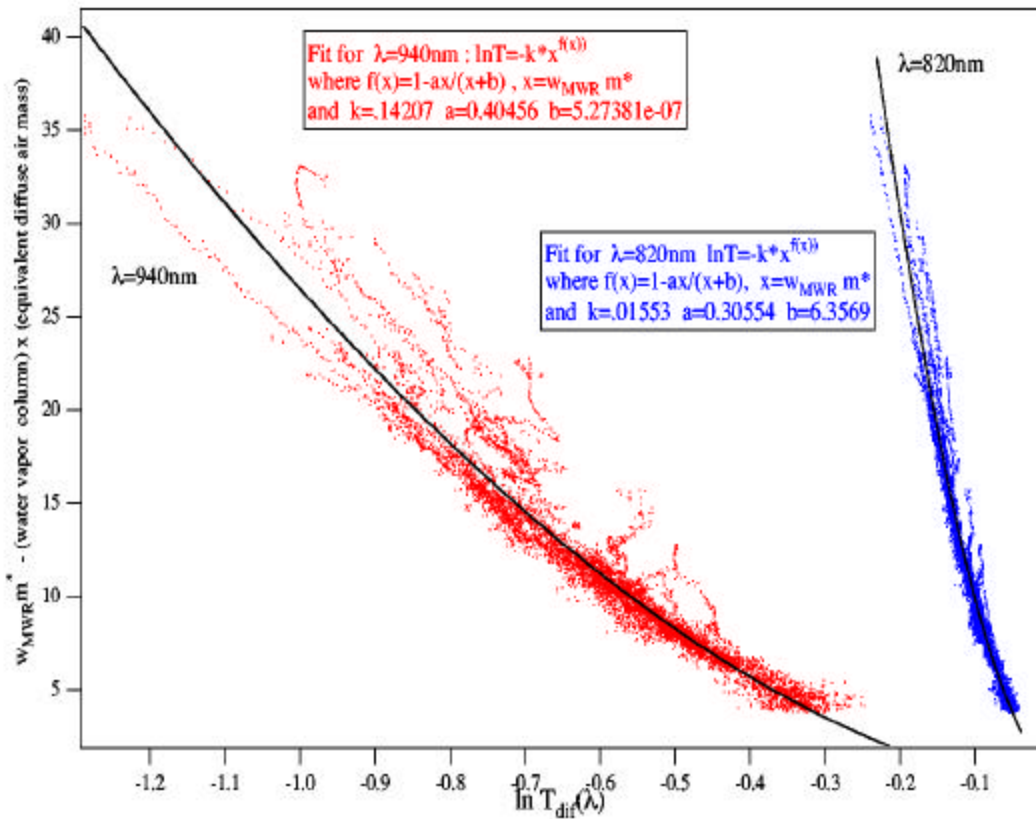


Figure 4. Derivation of effective diffuse curves of growth at 820 nm and 940 nm.

In this paper, we are chiefly concerned with the systematic errors as their magnitude determines the viability of our approach. The results indicate that during this IOP the retrievals of water vapor column from diffuse irradiance with rms error better than 0.24 mm are possible using a single empirical model for clear, semi-clear, and cloudy days. However, an objection can be raised that conditions during the IOP are not sufficiently representative of all possible climatological conditions. For instance, the surface albedo in March 1999 remained pretty constant due to snow coverage. One can imagine that parameters of the $h()$ may be different in summer when the albedo changes. Also, we did not analyze the prevailing type of cloud coverage during the overcast days. In particular, we do not know whether single-layer or multi-layer cloud conditions prevailed. The distinction between the two types of clouds is very important as photon pathlength changes dramatically between the two cloud conditions. Furthermore, in cases when the extra photon pathlength is accrued above the top of the water vapor profile, the expected reduction at 760-nm transmittance will not be congruent with the transmittance at water bands. Therefore, the compensation that function $g()$ in Eq. (7) is supposed to accomplish might be insufficient. These objections that are of a qualitative nature are important for designing a better scheme of retrieval; however, one must bear in mind that the success or failure of the retrieval method from the diffuse irradiance will be determined by the quantitative analysis, i.e., by the estimate of the systematic error $\bullet W_{\text{SYS}}$.

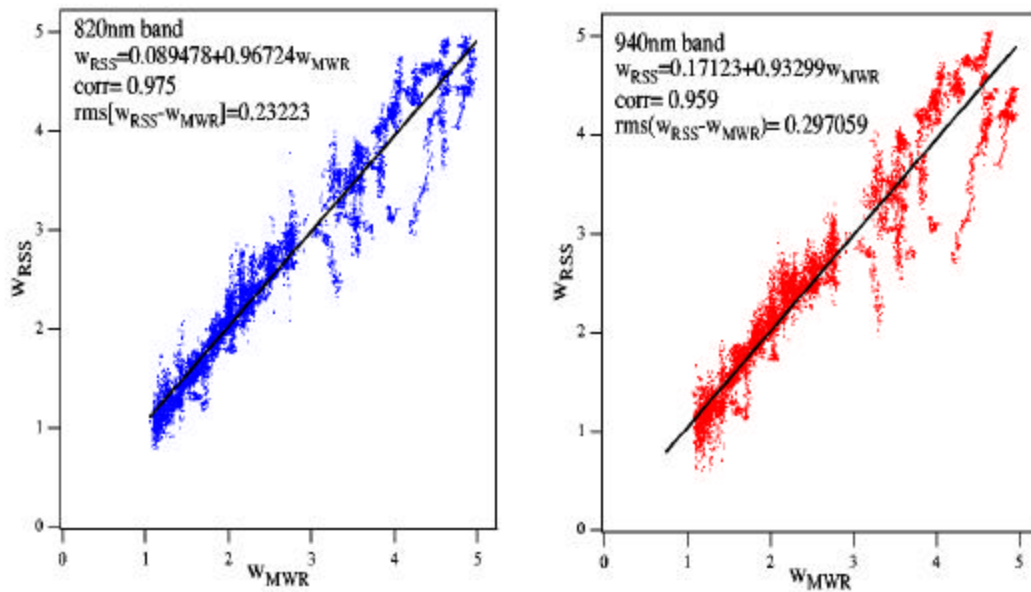


Figure 5. Correlation plots between RSS and MWR retrieved water vapor column.

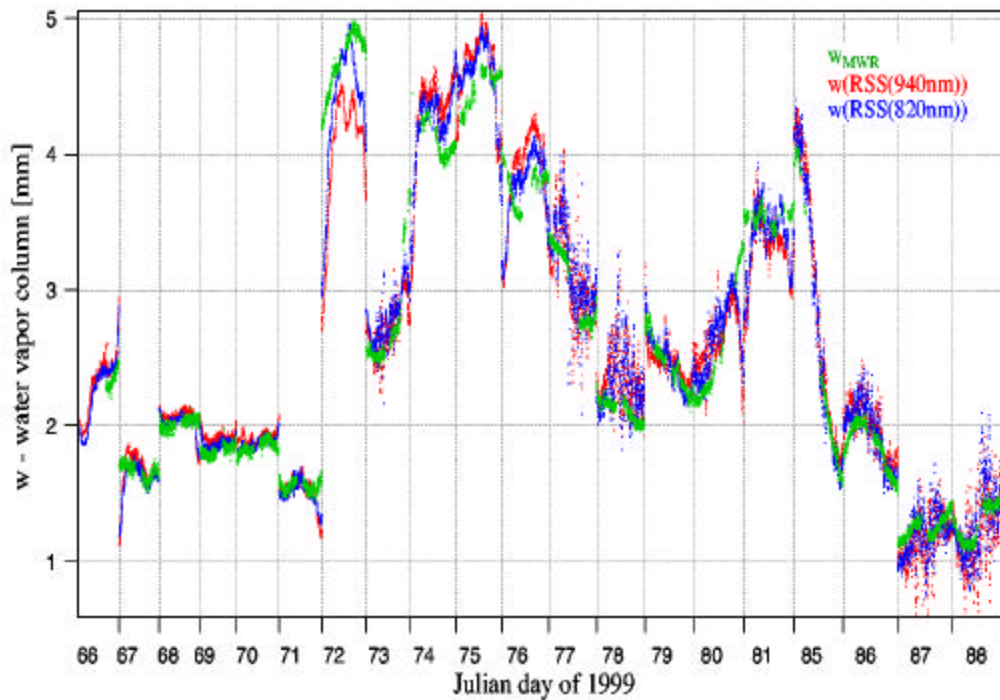


Figure 6. Water vapor column as function of time for 20 concatenated days.

The method presented is the simplest one among the ones that could take advantage of some information in the transmittance at the oxygen band. One is not limited to a method with the same parameters for both clear and overcast days. For instance, one may add an additional parameter of direct-diffuse ratio

$$r = \frac{1}{\cos(\text{SZA})} \frac{T_{\text{dir}}(781)}{T_{\text{dif}}(781)} \quad (11)$$

at a non-absorbing wavelength of 781-nm to distinguish between degree of overcast.

In Figure 7, along with the ratio r , a histogram of r values is plotted. The histogram suggests a division of data into four subgroups according to the values of r . One can improve the water vapor retrieval by generating a separate $h()$ function for each range of r . This is an additional parameterization of $h()$. While the improvement occurs, it is not large because the majority of all the outliers are within the same group ($0 < r < 4$). These are the points from the overcast days and points from the clear days at very large solar zenith angles. So, one could imagine adding explicit information on the solar zenith angle into the model to distinguish between the two types of low r points.

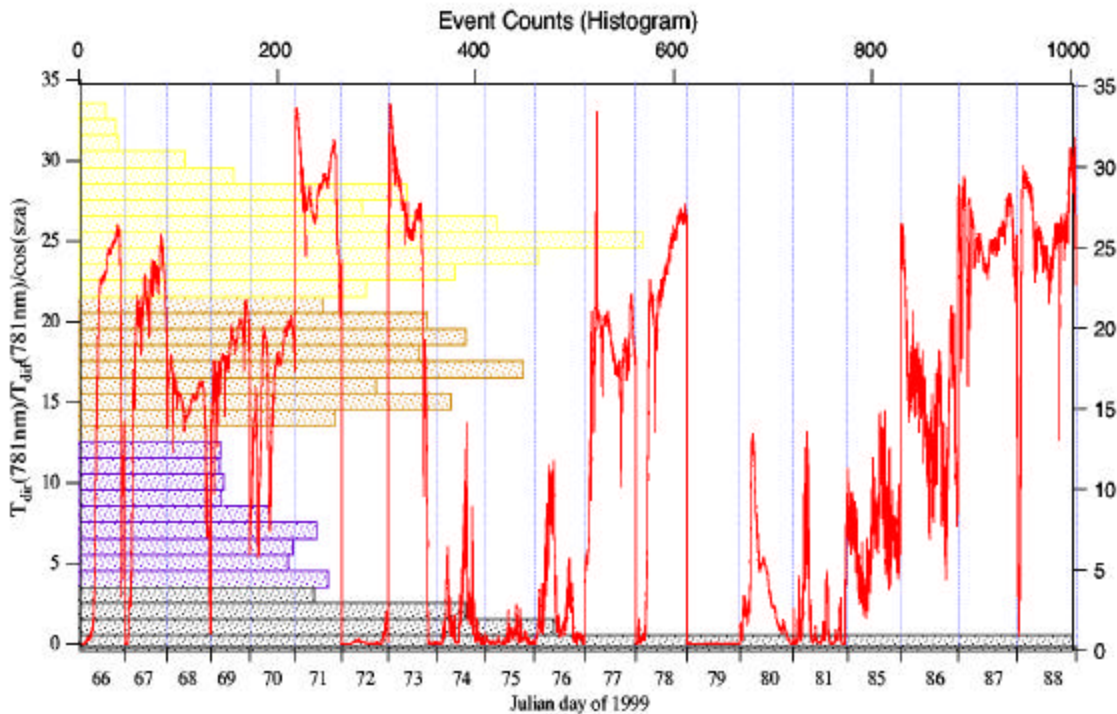


Figure 7. Direct-to-diffuse ratio at 781 nm and histogram of its values.

We can imagine further improvements by adding memory into the model. The presented model does retrievals instantaneously regardless of the preceding or succeeding results. The atmospheric and climatological changes occur in a finite time. For instance, changes of the surface albedo are gradual and they can be detected with more sophisticated tools such as the wavelength-dependent diffuse-to-direct ratio. The transmittance at 760 nm may contain some information about the type of the cloud coverage. For these reasons, we believe that retrievals from the diffuse irradiance of water vapor as well as other constituents such as ozone are promising and must be further investigated. Finally, we want to emphasize that all the possible improvements suggested in the previous two paragraphs would not utilize information beyond what the RSS is already providing.

Acknowledgments

The authors would like to thank Mark Beauharnois who helped with the RSS measurements and to Bernie Zak of Sandia National Laboratory and Knute Stamnes of the University of Alaska, Fairbanks who facilitated the deployment and operation of the RSS at the NSA site. This research was supported by the Environmental Sciences Division of the U.S. Department of Energy through grant number DE-FG02-90ER61072 (SUNY) as part of the ARM Program.

Corresponding Author

P. W. Kiedron, kiedron@asrc.cestm.albany.edu, (518) 437 8737

References

- Harrison, L., M. Beauharnois, J. Berndt, P. Kiedron, J. Michalsky, and Q. Min, 1999: The rotating shadowband spectroradiometer (RSS) at SGP. *Geophys. Res. Lett.*, **26**, 1715-1718.
- Kasten, F., 1965: A new table and approximation formula for relative air mass. *Arch. Meteor. Geophys. Bioklimatol. Ser. B*, **14**, 206-223.
- Kiedron, P., J. Michalsky, B. Schmid, D. Slater, J. Berndt, L. Harrison, P. Racette, E. Westwater, and Y. Han, 2001: A robust retrieval of water vapor column in dry arctic conditions using the rotating shadowband spectroradiometer. *J. Geophys. Research*. Submitted.
- Min, Q.-L., and L. Harrison, 1999: Joint statistics of photon pathlength and cloud optical depth. *Geophys. Res. Lett.* **26**, 1425-1428.
- Moskalenko, N. L., 1969: The spectral transmission function in the bands of water vapor, O₃, N₂O and N₂ atmospheric components. *Izv. Akad. Nauk. SSSR Fiz. Atmos. Okeana* **5**, 678.
- Pfeilsticker, K., F. Erle, O. Funk, H. Veitel, and U. Platt, 1998: First geometrical pathlengths probability density function derivation of the skylight from spectroscopically highly resolving oxygen A-band observations: 1. Measurement technique, atmospheric observations, and model calculations. *J. Geophys. Research*, **103**, 11,483-11,504.
- Racette, P., E. R. Westwater, Y. Han, W. Manning, A. Gasiewski, and D. C Jones, 2000: Millimeter-wave measurements of low amounts of precipitable water vapor. In *IGARSS'00*, July 24-28, 1154-1156.
- Veitel, H., O. Funk, C. Kurz, U. Platt, and K. Pfeilsticker, 1998: Geometrical path length probability density function of the skylight transmitted by mid-latitude cloudy skies; Some case studies. *Geophys. Res. Lett.*, **25**, 3355-3358.

Westwater, E. R., Y. Han, P. E. Racette, W. Manning, A. Gasiewski, and M. Klein, 2000: A comparison of clear-sky emission models with data taken during the 1999 Millimeter-Wave Radiometric Arctic Winter Water Vapor Experiment. In *Proceedings of the Tenth Atmospheric Radiation Measurement (ARM) Science Team Meeting*, U.S. Department of Energy, Washington, D.C. Available URL: [http://www.arm.gov/docs/documents/technical/conf_0003/westwater\(2\)-er.pdf](http://www.arm.gov/docs/documents/technical/conf_0003/westwater(2)-er.pdf)